

## CHAPTER 19

# *Modelling molecular conduction in DNA wires: charge transfer theories and dissipative quantum transport*

R. Bulla<sup>1</sup>, R. Gutierrez<sup>2</sup> and G. Cuniberti<sup>2</sup>

<sup>1</sup>*Theoretische Physik III, Universität Augsburg, D-86135, Augsburg, Germany*

<sup>2</sup>*Institut für Theoretische Physik, Universität Regensburg, D-93040, Regensburg, Germany*

## Abstract

Measurements of electron transfer rates as well as of charge transport characteristics in DNA have produced a number of seemingly contradictory results, ranging from insulating behaviour to the suggestion that DNA is an efficient medium for charge transport. Among other factors, environmental effects appear to play a crucial role in determining the effectivity of charge propagation along the double helix. This chapter gives an overview of charge transfer theories and their implication for addressing the interaction of a molecular conductor with a dissipative environment. Further, we focus on possible applications of these approaches for charge transport through DNA-based molecular wires.

## 19.1 INTRODUCTION

The discovery of long-range electron transfer processes in double stranded DNA [1] considerably attracted the attention of biologists, chemists and physicists. The motivation is threefold: (i) the possible use of DNA molecules in nanotechnology applications [2], (ii) the biological role of electron transfer in, for example, radiation damage and repair [3], and (iii) the potentials of biochemical sensors based on electron transfer in DNA [3].

Despite the intensive experimental efforts, the results for electron *transport* still appear to be contradictory, ranging from metallic conduction [4,5] to insulating behaviour with very large bandgaps [6,7]. We refer the reader to Ref. [8] for a recent review. The measurements of electron *transfer*, on the other hand, appear to be much better controlled and earlier discrepancies on the distance dependence of the electron transfer rate are now attributed to the different experimental set-ups [3].

1 Theoretically, several groups of factors have meanwhile been identified, which  
 2 considerably determine the effectivity of charge propagation along the double helix.  
 3 They can be roughly classified as being related to (i) static disorder associated with  
 4 the random or quasi-random sequence of bases in DNA oligomers [9–11], (ii) dy-  
 5 namical disorder arising from strong structural fluctuations of the molecular frame  
 6 [12–14], and (iii) environmental effects related to the presence of an aqueous envi-  
 7 ronment and counter-ions [15–21]. While the first two factors can still be addressed  
 8 in a first approximation by considering only the atomic structure of isolated DNA  
 9 oligomers, environmental effects require the consideration of the solvation shells and  
 10 counter-ions and their interaction with the DNA molecules. Though the performance  
 1 of *ab initio* approaches has considerably improved in recent years, the description of  
 2 the dynamical interaction of DNA with an environment is still a formidable computa-  
 3 tional task, involving several thousands of atoms. As a consequence, only relatively  
 4 few first-principle studies addressing this issue have been carried out in the recent  
 5 years [15–21]. Thus, model Hamiltonian approaches describing charge propagation  
 6 in the presence of a dissipative environment are very valuable and help to gain some  
 7 insight into the subtleties of the physical behaviour of a quantum mechanical system  
 8 interacting with a macroscopic number of degrees-of-freedom.

9 This chapter gives an overview of different approaches to address charge propagation  
 10 in a dissipative environment. In the next section, we discuss some results from *ab initio*  
 1 calculations of DNA oligomers in the presence of an aqueous environment. In Section  
 2 19.3 some basic facts on how to model the interaction between an arbitrary quantum me-  
 3 chanical system in interaction with a dissipative environment are introduced. Finally, in  
 4 Section 19.4, a special application to a DNA model is discussed.

## 7 19.2 ENVIRONMENTAL EFFECTS WITHIN *AB INITIO* APPROACHES

9 For the purposes of illustrating some basic facts concerning the electronic structure of a  
 10 *dried* DNA oligomer, let us look at a recent band-structure calculation of poly(GC) car-  
 1 ried out with density-functional-based code SIESTA [23]. First-principle results for  
 2 poly(AT) oligomers have also recently been presented [24–26]. The natural advantage of  
 3 poly(GC) is its periodic structure, which considerably minimizes the computational ef-  
 4 forts. In Fig. 19.1, the resulting band structure is shown. From the practical point of view,  
 5 it is also expected that this kind of periodic structure will have a higher potential appli-  
 6 cability in molecular electronics than their disordered counterparts like  $\lambda$ -DNA.

7 The topmost valence band (HOMO) and the lowest conduction band (LUMO), both  
 8 having  $\pi$ -character, are separated by a bandgap of  $\Delta = 2.0$  eV. The HOMO and LUMO  
 9 bands are basically derived from the overlap of guanine and cytosine orbitals, respec-  
 10 tively. As a consequence, the charge density of HOMO and LUMO bands is confined  
 1 along the G- and C-strands, respectively. The Fermi level lies between these two bands so  
 2 that the system appears to be an insulator.

3 Most striking are the very small bandwidths of the bands close to the Fermi level. The  
 4 topmost valence band has a width of  $W_H = 40$  meV while the lowest conduction band has  
 5 a somewhat broader bandwidth of  $W_L = 270$  meV. Part (b) of Fig. 19.2 of Ref. [23] (see

1  
2  
3  
4  
5  
6  
7  
8  
9  
10  
1  
2  
3  
4  
5  
6  
7  
8  
9  
20

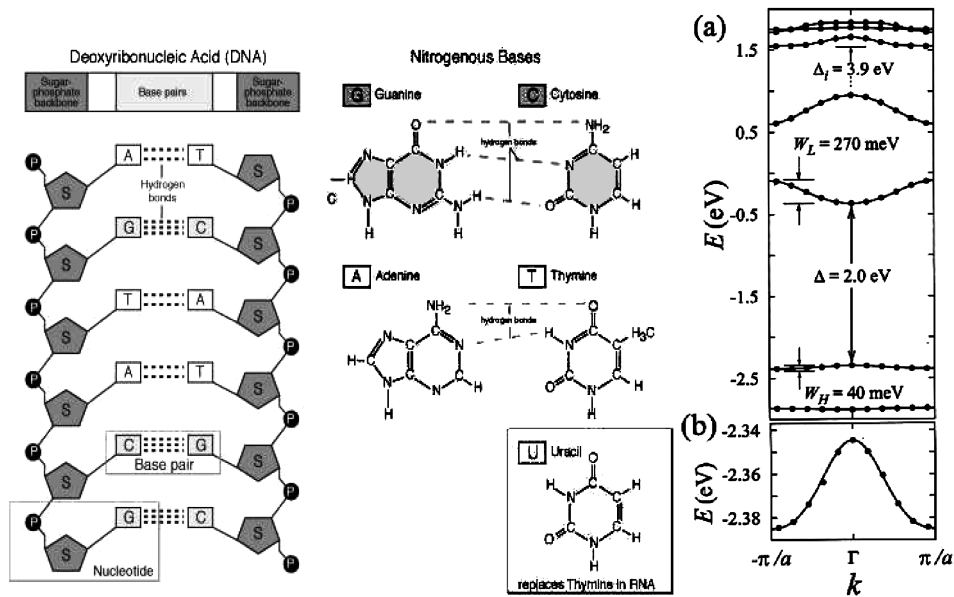


Fig. 19.1. Left: schematic representation of a double-stranded DNA oligomer with an arbitrary base-pair sequence. Right: electronic band-structure of poly(GC) DNA within density-functional theory. The figures are reproduced from Refs [22,23] with permission.

1  
2  
3  
4  
5  
6  
7  
8  
9  
30

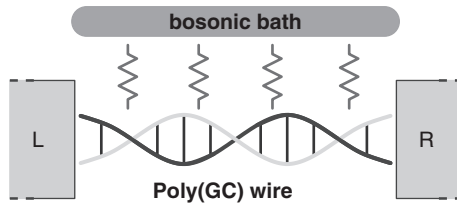


Fig. 19.2. Schematic representation of a double-stranded poly(GC) oligomer coupled to left (L) and right (R) electrodes and in interaction with a bosonic bath. The figure is reproduced from Ref. [37] with permission.

**AQ2**

1  
2  
3  
4  
5  
6  
7  
8  
9  
40  
41  
42  
43  
44  
45

Fig. 19.1, right panel, in this chapter) shows a tight-binding modelling of the topmost valence band using a single orbital per base pair. The resulting hopping matrix elements are  $t = 10$  meV (for nearest neighbour hopping) and  $t' = 1.5$  meV (for next-nearest neighbour hopping).

In principle, such a scenario allows for electronic transport mediated by carriers which are introduced by doping either in the top of the valence band or the bottom of the conduction band. The extremely small bandwidths, however, suggest that such a scenario cannot be stable under the various perturbations present in DNA [23].

One of the possible perturbations, which has been studied in some detail, is the role of the environment [15–19]. As shown in Ref. [15], the existence of rather different timescales of the environment may have a strong impact on a charge propagating along

1 the DNA molecule. First-principle simulations were performed, including four base  
 2 pairs of B-DNA in the sequence GAGG, together with Na counter-ions and the hydra-  
 3 tion shell. It turns out that holes can be gated by the temperature-dependent dynamics  
 4 of the environment, i.e., there may exist configurations that localize the hole.  
 5 Dynamical fluctuations of the counter-ions can lead, however, to configurations which  
 6 support hole motion. A hole thus experiences transitions between quantum-mechanical  
 7 states that are correlated with different environmental configurations [27]. These  
 8 results have been partly confirmed by recent *ab initio* simulations in Ref. [19]. The  
 9 authors have additionally pointed out at a different, proton-mediated mechanism for  
 10 hole localization, which may be quite effective in poly(GC) DNA.

1 The *ab initio*-based studies in Refs [16–18] have yielded further insight into the role  
 2 played by water and counter-ions in modifying the low-energy electronic structure of DNA  
 3 oligomers. Despite the differences in the DNA conformations (Z- [16] versus B-DNA  
 4 [17,18]) as well as in computational approaches (different basis sets and approximations  
 5 for the exchange-correlation potentials), they nevertheless indicate that the environment  
 6 can introduce midgap states. Though these electronic states do not form truly extended  
 7 electronic bands, they may support activated charge hopping at high temperatures and thus  
 8 lead to an enhancement of the conductivity. In this respect, they resemble, to some degree,  
 9 the defect levels induced by impurities in bulk semiconductors.

20 We can conclude from this that (i) the appearance of a bandgap is not at all a generic  
 1 feature for the bandstructure of DNA, and (ii) the extremely small values of the bandwidths  
 2 do appear to be generic. The general question which arises from that is the relation of the  
 3 bandwidths  $W_H$  and  $W_L$  to other typical energy scales due to disorder effects,  
 4 electron–phonon coupling, and Coulomb correlations. Furthermore, the environment can  
 5 have a dramatic influence on the electronic structure of the oligomer by inducing defect-  
 6 like states within the  $\pi - \pi^*$  gap. However, as previously stated, the complexity of the prob-  
 7 lem makes a full *ab initio* treatment rather difficult. This leads us to the issue of how the  
 8 system – environment interaction can be modelled within a Hamiltonian model approach.  
 9 Which are the essential ingredients that have to be taken into account?

30

1

2

3

### 19.3 MODELLING THE SYSTEM–ENVIRONMENT INTERACTION

4

5

6

7

8

9

10

11

12

13

14

15

16

17

18

19

20

21

22

23

24

The importance of the system–environment interaction has long been recognized in bio-  
 molecules (such as proteins), in which electron transfer reactions take place. Within Marcus  
 theory [28], the coupling of the electronic degrees-of-freedom to a reaction coordinate is  
 the first step to a successful description of electron transfer processes. The quantum-  
 mechanical analogue of the reaction coordinate is a phononic degree-of-freedom originat-  
 ing from vibrations of the protein matrix. In general, there might not be one dominating  
 phononic mode; such a breakdown of the standard single reaction coordinate description  
 has been suggested in the context of charge transfer between DNA base pairs [29]. More  
 importantly, even a dominating reaction coordinate is coupled to the fluctuations of the  
 environment, such as surrounding water molecules, so that the resulting spectral function  
 $J(\omega)$  of all relevant phononic modes can be regarded as continuous over a very broad en-  
 ergy range (in theoretical calculations, the low-energy cut-off is typically set to  $\omega = 0$ ).

1 The coupling of the electronic subsystem (the electron transferred between donor and  
2 acceptor site) to the environment leads to a very important effect: when an electron ini-  
3 tially localized at the donor site, tunnels to the acceptor site (which typically has a lower  
4 energy), the energy difference is dissipated to the environment so that the electron trans-  
5 fer process is irreversible [30]. If this friction were to be too small, or if the electron were  
6 to couple to a single phonon mode only, the electron would oscillate between donor and  
7 acceptor sites, making the electron transfer process highly inefficient.

8 In the work of Garg *et al.* [30], the friction term has been modelled quantum me-  
9 chanically via a coupling to a bath of harmonic oscillators. A minimal model for electron  
10 transfer processes, similar to the one proposed in [30], then takes the form:

$$\begin{aligned}
 1 \quad H = & \sum_{i=A,D} \varepsilon_i c_i^\dagger c_i - t (c_D^\dagger c_A + c_A^\dagger c_D) \\
 2 & + \sum_n \omega_n b_n^\dagger b_n + (g_A n_A + g_D n_D) \sum_n \frac{\lambda_n}{2} (b_n^\dagger + b_n) \quad (1)
 \end{aligned}$$

7 The operators  $c_i^{(\dagger)}$  denote annihilation (creation) operators for electrons on the donor ( $i =$   
8 D) and acceptor ( $i = A$ ) sites;  $n_{A/D}$  is defined as  $n_i = c_{i\sigma}^\dagger c_{i\sigma}$ . The first two terms of the  
9 Hamiltonian, Eq. (1), correspond to a two-site tight-binding Hamiltonian with  $\varepsilon_i$  the on-  
10 site energies and  $t$  the hopping matrix element.

1 The last two terms in Eq. (1) describe the free bosonic bath (with bosonic creation  
2 and annihilation operators  $b_n^\dagger$  and  $b_n$ ) and the coupling between electrons and bosons, re-  
3 spectively. Assuming symmetric phonon displacements due to the electronic occupancy  
4 at donor and acceptor sites, one can set  $g_A = 1$  and  $g_D = -1$  see Ref. [31].

5 The coupling of the electrons to the bath degrees-of-freedom is completely specified  
6 by the bath spectral function  $J(\omega) = \pi \sum_n \lambda_n^2 \delta(\omega - \omega_n)$ . The form of  $J(\omega)$  can, in princi-  
7 ple, be calculated with molecular dynamics simulations (see, for example, [32]). To study  
8 the qualitative influence of the environment, an ohmic bath spectral function  $J(\omega) \propto \omega$   
9 (with a suitable high-energy cut-off) is sufficient for most cases. In this description, dom-  
10 inant reaction coordinates lead to additional resonances in the bath spectral function.

1 Note that such a continuous bath spectral function enforces a *quantum-mechanical*  
2 treatment of the phononic degrees-of-freedom, since the temperature range always lies  
3 within the continuum of phononic modes.

4 The Hamiltonian, Eq. (1), can be viewed as a paradigm for modelling the system-  
5 environment interaction in biomolecules in which the electronic degrees-of-freedom  
6 couple to a dissipative environment. We should add here that the model, Eq. (1), can  
7 be exactly mapped onto the well-studied spin-boson model [33,34] for the case of *one*  
8 electron in the system. In the spin-boson model description, the state  $|\uparrow\rangle$  ( $|\downarrow\rangle$ ) corresponds  
9 to the electron localized at the donor (acceptor) site. More complicated situations arise  
10 when the spin degree-of-freedom of the electron — not to be confused with the artifi-  
11 cial spin in the spin-boson model — is taken into account, see the discussion in [35].

12 Calculations for these types of models in the context of electron transfer problems  
13 have been presented in [30,35,36]. Let us now move on to the topic of this chapter, elec-  
14 tron transport in DNA. It is natural to assume that the electron environment interaction  
15 plays an equally important role for electron transport through the DNA double helix. The

1 main difference here is that electron transfer/transport occurs over very many sites so that  
 2 the two-site model, Eq. (1), has to be suitably generalized. One such example is dis-  
 3 cussed in the following section.

#### 6 **19.4 MODELLING THE SYSTEM-ENVIRONMENT INTERACTION:** 7 **A DNA-WIRE IN A DISSIPATIVE BATH**

8  
 9 The first-principle calculations reviewed in Section 19.1 have shown that the environ-  
 10 ment in which DNA oligomers are placed may have a non-negligible influence on their  
 1 electronic structure. In this section, we will illustrate within an effective model  
 2 Hamiltonian approach, how the presence of a dissipative environment does affect the  
 3 low-energy transport properties of a DNA molecular wire [38,39]. Our reference system  
 4 will be poly(GC) because of its periodic structure, which should make optimal the inter-  
 5 base electronic coupling along the strands. Moreover, recent experiments [40] on single  
 6 poly(GC) molecules have shown non-zero current at low bias, which is at variance with  
 7 the fact that the molecule should have a (rather large) HOMO-LUMO gap [41]. Since  
 8 these experiments were performed in an aqueous environment and the authors excluded  
 9 ionic current contributions, one may consider the possibility that the environment is mod-  
 10 ifying the molecule's electronic structure.

1 In our model, we will exclusively focus on the low-energy transport, i.e., the charge  
 2 injection energies are small compared with the molecular bandgap of the isolated mole-  
 3 cule ( $\sim 2 - 3$  eV). Consequently, only equilibrium transport will be considered and a  
 4 transmission-like function can still be defined [38,39,42]. At low energies, only the  
 5 frontier orbitals (HOMO and LUMO) of the molecule are expected to contribute to trans-  
 6 port. As mentioned in section 19.1 these orbitals have  $\pi$ -character and their charge den-  
 7 sities extend along the G- and C-strands for the HOMO and the LUMO, respectively.  
 8 Motivated by this, we have formulated a minimal tight-binding model [38,39,43], where  
 9 a single electronic  $\pi$ -orbital channel is connected to left and right electrodes. The  
 10 sugar-phosphate backbones are assumed to locally perturb the electronic states and lead  
 1 to the opening of a semiconducting gap for the infinite chain. As a result, the size of the  
 2 bandgap can be controlled by the strength of this perturbation, given by the parameter  $t_{\perp}$   
 3 in Eq. (2) below. The environment is described by a collection of harmonic oscillators  
 4 which linearly couple to the charge density on the backbone sites. Assuming zero on-site  
 5 energies (the Fermi level thus lies at  $E = 0$ ), the Hamiltonian reads:

$$\begin{aligned}
 \mathcal{H} &= -t_{\pi} \sum_j [c_j^{\dagger} c_{j+1} + h.c.] - t_{\perp} \sum_j [b_j^{\dagger} c_j + h.c.] \\
 &+ \sum_{\alpha} \Omega B_{\alpha}^{\dagger} B_{\alpha} + \sum_{\alpha, j} \lambda_{\alpha} b_j^{\dagger} b_j (B_{\alpha} + B_{\alpha}^{\dagger}) \\
 &+ \sum_{k \in L, R, \sigma} \epsilon_{k\sigma} d_{k\sigma}^{\dagger} d_{k\sigma} + \sum_{k \in L, \sigma} (V_{k,1} d_{k\sigma}^{\dagger} c_1 + h.c.) + \sum_{k \in R, \sigma} (V_{k,N} d_{k\sigma}^{\dagger} c_N + h.c.) \\
 &= \mathcal{H}_{cl} + \mathcal{H}_B + \mathcal{H}_{leads} \quad (2)
 \end{aligned}$$

1 In the above equation,  $\mathcal{H}_{\text{el}} = \mathcal{H}_{\text{c}} + \mathcal{H}_{\text{b}}$  is the Hamiltonian of the HOMO (or LUMO)  
 2 channel ( $\mathcal{H}_{\text{c}}$ ) and the backbone sites ( $\mathcal{H}_{\text{b}}$ );  $\mathcal{H}_{\text{b}}$  contains both the Hamiltonian of the bath  
 3 and the mutual interaction of the bath with the electronic degrees-of-freedom at the back-  
 4 bone sites (second row). Finally,  $\mathcal{H}_{\text{leads}}$  contains the electrode Hamiltonians as well as the  
 5 tunnelling Hamiltonian describing the propagation of a charge from the leads onto the  
 6 HOMO (or LUMO) channel and vice versa. In the absence of coupling to the bath, the  
 7 eigenstates of  $\mathcal{H}_{\text{el}}$  yield two manifolds containing  $N$  states each and separated by a  
 8 bandgap, whose magnitude basically depends on the size of the transversal coupling  $t_{\perp}$ .  
 9 The bath is completely described by introducing its spectral density as given by [34]:  
 10  $J(\omega) = J_0 \left(\frac{\omega}{\omega_c}\right) \exp^{-\omega/\omega_c}$ , where  $\omega_c$  is a high-frequency cut-off and we assume ohmic  
 1 dissipation,  $J(\omega) \sim \omega$ , see also the previous section. By performing a unitary transforma-  
 2 tion, the linear coupling to the bath can be eliminated. However, the transversal coupling  
 3 terms will be renormalized by exponential bosonic operators [38,39]. Using equation of  
 4 motion techniques, one can show, to lowest order in  $t_{\perp}$ , that the Green function of the wire  
 5 satisfies the following Dyson equation:  
 6

$$7 \quad \mathbf{G}^{-1}(E) = E\mathbf{1} - \mathcal{H}_{\text{c}} - \Sigma_{\text{L}}(E) - \Sigma_{\text{R}}(E) - t_{\perp}^2 \mathbf{P}(E) \quad (3)$$

8 In this expression, the influence of the electrodes is captured by the complex self-energy  
 9 functions  $\Sigma_{\text{L/R}}(E)$ . The function  $P(E)$  is an entangled electron-boson Green function:  
 10

1  $P_{ji}(t) = -i\Theta(t) \langle [b_j(t)\chi(t), b_i^{\dagger}(0)\chi^{\dagger}(0)] \rangle$  and  $\chi = \exp[\sum_{\alpha}(\lambda_{\alpha}/\Omega_{\alpha})(B_{\alpha}B_{\alpha}^{\dagger})]$ . Note that  $P(E)$   
 2 acts as an additional self-energy and that the influence of the backbones is contained only  
 3 in this function.  
 4

5 Several coupling regimes to the bath can be analysed [39]. We focus here only on  
 6 the strong-coupling limit (SCL), defined by the condition  $J_0/\omega_c > 1$ , which basically  
 7 means that the timescales of the charge-bath interaction are much shorter compared  
 8 with typical electronic timescales. We refer the reader to Refs. [38,39] for technical  
 9 details.

10 The impact of the bath on the electronic structure is twofold [38,39]. On one side, the  
 1 strong coupling to the bath leads to the emergence of new bath-induced electronic states  
 2 *inside* the wire bandgap. On the other side, however, these states are strongly damped by  
 3 the dissipative action of the bath. In other words, the bath completely destroys the coher-  
 4 ence of transport through the wire. This effect has also been discussed for transport  
 5 through molecular chains under the influence of external time-dependent fields, see  
 6 [44,45]

7 As a result, the bath-induced states will not manifest as resonances in the transmission  
 8 spectrum, see Fig. 19.3, left panel. Nevertheless, they induce a *temperature dependent*  
 9 background, which leads to a (small) finite density of states inside the gap. Charges in-  
 10 jected at low energies will now find states supporting transport at high temperatures and  
 1 thus, a finite current at low bias may flow. Hence, we call the new gap a pseudo-gap, in  
 2 contrast to the intrinsic bandgap found in the isolated wire. Note that increasing the in-  
 3 teraction with the bath (increasing  $J_0/\omega_c$ ) does not necessarily lead to a global increase of  
 4 the current, since the frontier orbitals of the wire are strongly damped with increasing  
 5 coupling.  
 6

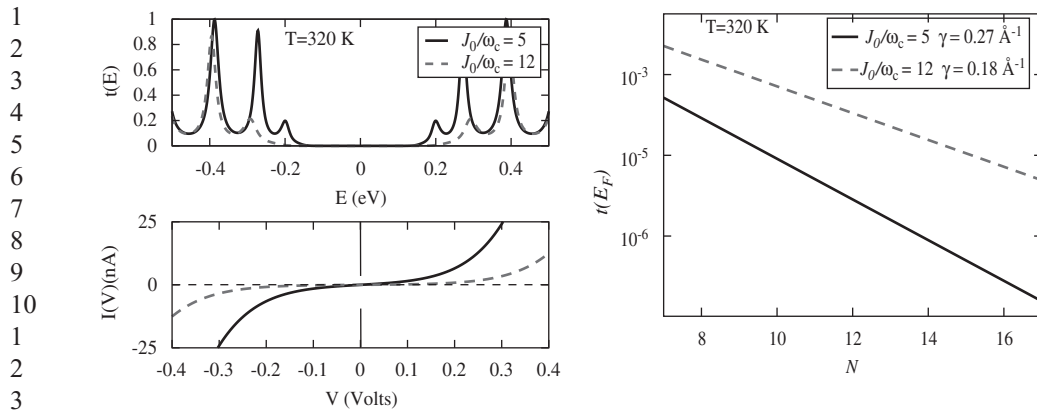


Fig. 19.3. Strong coupling limit. Left panel: transmission and current for different electron–boson coupling strengths. At high temperatures, a small density of states is present at low energies. Right panel: corresponding dependence of the transmission at the Fermi energy on the number of sites  $N$  in the wire. A very weak exponential scaling is found, hinting at a strong contribution of incoherent processes.

Signatures of this situation are seen in the length dependence of the transmission at the Fermi energy, see Fig. 19.3, right panel. Tunnelling through an intrinsic gap would lead to a very strong exponential length dependence  $t(E_F) \sim e^{-\gamma N}$  with an inverse decay length  $\gamma \sim 1.5 - 2 \text{ \AA}^{-1}$  [41]. We find, however, much smaller values  $\sim 0.1 - 0.2 \text{ \AA}^{-1}$ . With increasing bath coupling the exponential dependence weakens, reflecting the increase of the density of states in the pseudo-gap and the strong contribution of incoherent processes [46].

## 19.5 OUTLOOK

One of the major problems for the theoretical modelling of charge transport in DNA oligomers is the lack of a clear experimental picture of their transport signatures. Thus, focusing on individual factors affecting charge propagation helps to shed light onto the relevant mechanisms controlling the charge dynamics in DNA. We have addressed in this chapter environmental effects in the charge transport through DNA oligomers within a minimal Hamiltonian model approach. Obviously, other factors not treated here, like electronic correlations, static disorder or internal vibrational excitations can also have a non-negligible influence on charge propagation.

## 19.6 ACKNOWLEDGEMENTS

The authors thank A. Nitzan for useful comments and suggestions. This research was supported by the DFG through SFB 484, by the Volkswagen Foundation and by the EU under contract IST-2001-38951.

## 19.7 REFERENCES

- 1 C.J. Murphy, M.R. Arkin, Y. Jenkins, N.D. Ghatlia, S.H. Bossmann, N.J. Turro and J.K. Barton, *Science* 262 (1993) 1025.
- 2 C. Dekker and M. Ratner, *Physics World*, August 2001.
- 3 E.M. Boon and J.K. Barton, *Curr. Op. in. Struct. Biol.*, 12 (2002) 320.
- 4 H.-W. Fink and C. Schönberger, *Nature*, 398 (1999) 407.
- 5 A.Y. Kasumov, M. Kociak, S. Guron, B. Reulet, V. T. Volkov, D.V. Klinov and H. Bouchiat, *Science*, 291 (2001) 280.
- 6 D. Porath, A. Bezryadin, S.D. Vries and C. Dekker, *Nature*, 403 (2000) 635.
- 7 A.J. Storm, J.V. Noort, S.D. Vries and C. Dekker, *Appl. Phys. Lett.*, 79 (2001) 3881.
- 8 D. Porath, G. Cuniberti and R. Di Felice, *Topics Curr. Chem.*, 237, (2004) 183.
- 9 S. Roche, D. Bicut, E. Macia and E. Kats, *Phys. Rev. Lett.*, 228101 (2003).
- 10 S. Roche, *Phys. Rev. Lett.*, 91 (2003) 108101.
- 11 D. Klotsa, R.A. Röemer and M. S. Turner, q-bio.GN/0504004, 2005.
- 12 F. Palmero, J.F.R. Archilla, D. Hennig and F.R. Romero, *New J. Phys.*, 6 (2004) 13.
- 13 S. Komineas, G. Kalosakas and A.R. Bishop, *Phys. Rev. E*, 65 (2002) 061905.
- 14 F.C. Grozema, L.D.A. Siebbeles, Y.A. Berlin and M.A. Ratner, *Chem. Phys. Chem.*, 6 (2002) 536.
- 15 R.N. Barnett, C.L. Cleveland, A. Joy, U. Landman and G. B. Schuster, *Science*, 294 (2001) 567.
- 16 F.L. Gervasio, P. Carolini and M. Parrinello, *Phys. Rev. Lett.*, 89 (2002) 108102.
- 17 R.G. Endres, D.L. Cox and R.R.P. Singh, *Rev. Mod. Phys.*, 76 (2004) 195.
- 18 A. Hübsch, R.G. Endres, D.L. Cox and R.R.P. Singh, *Phys. Rev. Lett.*, 94 (2005) 178102.
- 19 F.L. Gervasio, A. Laio, M. Parrinello and M. Boero, *Phys. Rev. Lett.*, 94 (2005) 158103.
- 20 Ch. Adessi, S. Walch and M.P. Anantram, *Phys. Rev. B*, 67 (2003) 081405(R).
- 21 H. Mehrez and M.P. Anantram, *Phys. Rev. B*, 71 (2005) 115405.
- 22 <http://www.accessexcellence.org/RC/VL/GG/>; <http://www.genome.gov/>.
- 23 E. Artacho, M. Machado, D. Sanchez-Portal, P. Ordejon and J.M. Soler, *Mol. Phys.*, 101 (2003) 1587.
- 24 E.B. Starikov, *Phys. Chem. Chem. Phys.*, 4 (2002) 4523.
- 25 J.P. Lewis, J. Picus, Th. E. Cheatham III, E.B. Starikov, H. Wang, J. Tomfohr and O.F. Sankey, *Phys. Stat. Solidis B*, 223 (2002) 90.
- 26 J.P. Lewis, Th. E. Cheatham III, E.B. Starikov and O.F. Sankey, *J. Phys. Chem. B*, 107 (2003) 2581.
- 27 We note that a similar situation is known in electron transfer theories, where solvent reorganization brings into resonance the electronic states of donor and acceptor centres.
- 28 R.A. Marcus, *J. Chem. Phys.*, (1956) 966; *Rev. Mod. Phys.*, 65 (1999) 599.
- 29 R. Bruinsma, G. Gruener, M.R. D'Orsogna and J. Rudnick, *Phys. Rev. Lett.*, 85 (2000) 4393.
- 30 A. Garg, J. N. Onuchic and V. Ambegaokar, *J. Chem. Phys.*, 83 (1985) 4491.
- 31 V. May and O. Kühn, *Charge and Energy Transfer Dynamics in Molecular Systems*, WI-VCH, Weinheim, 2004.
- 32 D. Xu and K. Schulten, *Chem. Phys.*, 182 (1994) 91.
- 33 A.J. Leggett, S. Chakravarty, A.T. Dorsey, M.P.A. Fisher, A. Garg and W. Zwerger, *Rev. Mod. Phys.*, 59 (1987) 1.
- 34 U. Weiss, *Quantum Dissipative Systems*, Vol. 10 of Series in Modern Condensed Matter Physics, World Scientific, 1999.
- 35 S. Tornow, N.-H. Tong and R. Bulla, cond-mat/0502276, 2005.
- 36 L. Mühlbacher and R. Egger, *Chem. Phys.*, 296 (2004) 193.
- 37 <http://pubs.acs.org/journals/nalefd/index.html>.
- 38 R. Gutierrez, S. Mandal and G. Cuniberti, *Nano Lett.*, 5 (2005) 1093.
- 39 R. Gutierrez, S. Mandal and G. Cuniberti, *Phys. Rev. B*, 71 (2005) 235116.
- 40 B. Xu, P. Zhang, X. Li and N. Tao, *Nano Lett.*, 4 (2004) 1105.
- 41 H. Wang, J. P. Lewis and O. Sankey, *Phys. Rev. Lett.*, 93 (2004) 016401.
- 42 Y. Imry, O. Entin-Wohlman and A. Aharony, cond-mat/0409075, 2004.
- 43 G. Cuniberti, L. Craco, D. Porath and C. Dekker, *Phys. Rev. B*, 65 (2002) 241314(R).
- 44 J. Lehmann, S. Kohler, V. May and P. Hänggi, *J. Chem. Phys.*, 121 (2004) 2278.
- 45 S. Kohler, J. Lehmann and P. Hänggi, *Phys. Rep.*, 406 (2005) 397.
- 46 D. Segal, A. Nitzan, W. B. Davis and M.A. Ratner, *J. Phys. Chem.*, 104 (2000) 2790; D. Segal and A. Nitzan, *Chem. Phys.*, 281 (2002) 235.

AQ3

AQ1

